FINAL-FOCUS SCHEMES FOR CLIC AT 3 TEV

F. Zimmermann, H. Burkhardt, T. Risselada, F. Schmidt, CERN, Geneva, Switzerland,
H.-J. Schreiber, DESY Zeuthen, Germany

Abstract

We discuss benefits and drawbacks of two different final-focus schemes for CLIC at 3 TeV centre-of-mass (c.m.) energy, by examining tolerances, tunability and potential background for a 3.3-km long baseline final-focus system [1] and a shorter advanced design [2].

1 INTRODUCTION

The length of the final-focus system may have a significant impact on the total extent of a 3-TeV CLIC. We here compare the 3.3-km long baseline optics [1] with a more compact system developed by Raimondi [2]. In particular, we discuss performance, tolerances, collimation, and tunability of these two systems.

2 OPTICS

The baseline optics was described in Ref. [1]. Beta functions and dispersion of the alternative compact optics are depicted in Fig. 1.

The baseline optics [1] is a rather conventional, modular design, consisting of matching section, horizontal chromatic correction, vertical chromatic correction, and final transformer. Two pairs of sextupoles correct the doublet chromaticity. The sextupoles of a pair are separated by an optical $-I$ transform, so that geometric aberrations cancel. Following a proposal by Oide [3], the dispersion is nonzero only at the second sextupole of each pair. This reduces the number of bending magnets, hence the synchrotron radiation, and also the chromo-geometric aberrations. Second order dispersion is corrected by adjusting the ratio of bending angles in the two chromatic correction sections.

The second optics derives from the NLC 1-TeV final focus, developed by Raimondi and Seryi [2]. To limit the impact of synchrotron radiation, the sextupole strengths were increased by a factor 3.4 from the NLC design and all bending angles reduced accordingly. Upstream quadrupoles, sextupoles, and bending angles have been empirically fine-tuned for maximum luminosity, using a Monte-Carlo optimization. This optics is only 500 m long. The dispersion has a nonzero slope at the collision point ($D_x'^* = 1.8$ mrad), and is maximum across the final doublet. Two sextupoles are located here. Three other sextupoles are positioned upstream of the main bending magnets. They cancel the geometric aberrations induced by the two chromatic sextupoles. The free length between the exit face of the last quadrupole and the collision point, l^*, is 4.3 m, compared with 2 m for the first optics. This leaves more space for the detector and it would avoid placing final quadrupoles inside the detector solenoid field.

Table 1 lists relevant parameters for the two systems. The gradient of the last sextupole in the compact system would correspond to a pole-tip field of about 2 T at 5 mm radius. The length of this magnet could be doubled from 0.6 to 1.2 m, without introducing significant aberrations.

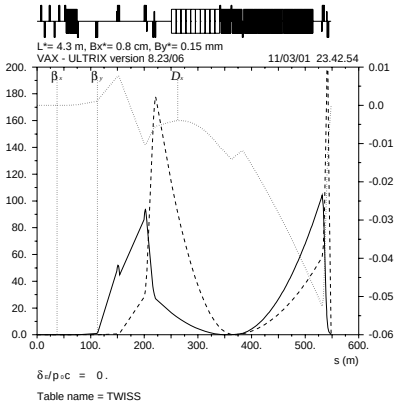

Figure 1: Compact final focus scaled from the NLC design [2]. Beta-function values on the left axis are in units of km, dispersion values on the right are in m. The interaction point (IP) is on the right.

Table 1: Beam and final-focus parameters.

optics	baseline	compact
beam energy	1.5 TeV	
no. of bunches per second	15400	
bunch population	4×10^9	
ideal luminosity w/o pinch	4.56×10^{34} cm^{-2}s^{-1}	
IP beta functions	8.0 (x), 0.15 (y) mm	
IP normalized emittances	0.68(x), 0.02 (y) μm	
full-width momentum spread	0.8–1.0%	
demagnification factor	90 (x), 346 (y)	
peak vertical beta function	1000 km	200 km
peak dispersion	10 cm	5 cm
total length	3282 m	548 m
total bending length	705 m	276 m
total bending angle $\sum \lvert\theta_i\rvert$	586 μrad	363 μrad
gradient of last quadrupole	450 T/m	388 T/m
gradient of 2nd last quadr.	184 T/m	135 T/m
strength of SD sextupole	1.29 m^{-3}	20.1 m^{-3}
strength of SF sextupole	2.70 m^{-3}	5.6 m^{-3}

3 PERFORMANCE

Figures 2 and 3 display the luminosity simulated with and without synchrotron radation as a function of the beam energy spread for the two final-focus systems. The luminosity was computed by convoluting tracked particles on a grid. Figure 4 shows the corresponding rms beam sizes, for the case with synchrotron radiation. All figures depict simulation results from MAD [4] and from Sixtrack90 [5]. The

latter is an operator-overloaded Fortran90 upgrade of Sixtrack [6], and is believed to represent higher-order chromatic effects more accurately than MAD.

The luminosity for nominal parameters (0.8% full energy spread) is about the same for the two optics. Figures 2 and 3 identify synchrotron radiation as the dominant limitation, which reduces the luminosity to 65–75% of the ideal value. The energy bandwidth of the compact system is wider, and would allow maintaining a larger BNS damping at the end of the linac.

Residual optical aberrations were analyzed using automatic differentiation in Sixtrack90; see Table 2.

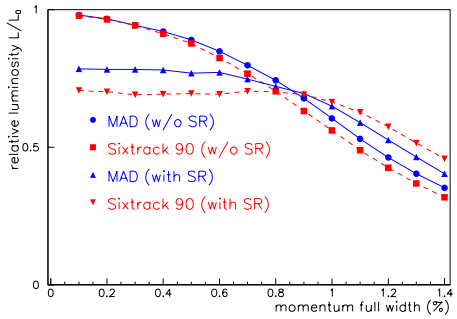

Figure 2: Luminosity, in units of the ideal geometric luminosity L_0, vs. the full-width momentum spread for the baseline optics, as simulated by MAD [4] and Sixtrack90 [6] with and without synchrotron radiation.

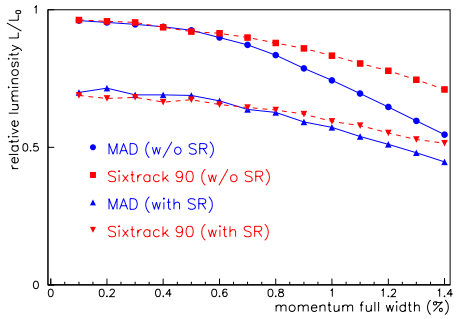

Figure 3: Relative luminosity vs. the full-width momentum spread for the compact optics, as simulated by MAD [4] and Sixtrack90 [6] including random energy fluctuations due to synchrotron radiation.

Table 2: Residual aberrations $\Delta\sigma_{x(y)}/\sigma_{y(x),0}$, which are added in quadrature to the linear spot sizes $\sigma_{y(x),0}$.

	Lie gen.	$\Delta\sigma_x/\sigma_{x0}$	Lie gen.	$\Delta\sigma_y/\sigma_{y0}$
baseline	$x'^4\delta$	0.70	$y'^2\delta^2$	0.41
	$x'^2\delta^3$	0.43	$x'y'^2\delta^2$	0.15
	$x'^2\delta^2$	0.40	$y'^2\delta^3$	0.12
compact	$x'\delta^2$	0.42	$y'^2\delta$	0.91
	$x'^2\delta$	0.41	$x'^2y'^2\delta$	0.31

The tunability of the two system is comparable: Varying β_x^* from 10 mm to 2 mm, decreases the luminosity, in units

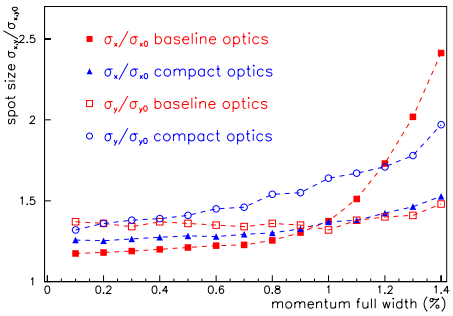

Figure 4: Horizontal and vertical rms beam sizes simulated by Sixtrack90 [6] including synchrotron radiation vs. the full-width momentum spread for the two optics.

of ideal luminosity, from 71% to 25% for the baseline, and from 66% to 31% for the compact optics. Jitter and drift tolerances on vertical magnet positions and field strength are similar as well.

Figure 5 shows that the transverse tails at the entrance to the final quadrupole are much smaller for the compact system, thus reducing an important background source.

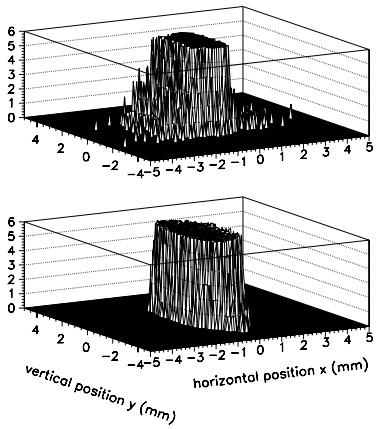

Figure 5: Beam halo at final-quadrupole entrance for baseline (top) and compact optics (bottom). The initial (uniform) distribution extends up to $\pm 15\sigma_x$, $\pm 70\sigma_y$, and $\pm 4\%$.

4 COLLIMATION ISSUES

The beams in a linear collider must be collimated before passing through the final doublet. The collimation depth is determined from the conditions that (1) beam particles and (2) synchrotron radiation photons should not hit any magnet apertures on the incoming side of the IP. Figures 6 and 7 show synchrotron radiation fans emitted in the final doublet. The collimation depth for the baseline optics should be less than $23\sigma_x$ and $80\sigma_y$ and that for the compact optics less than $14\sigma_x$ or $83\sigma_y$. In the latter case the horizontal beam size σ_x includes both betatron and dispersive components, of roughly equal size. The horizontal betatron collimation depth required is about half that of the baseline.

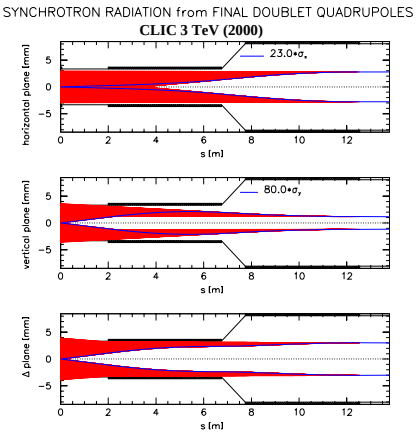

Figure 6: Synchrotron radiation fans across the final doublet for the baseline optics with beam envelopes of $23\sigma_x$ and $80\sigma_y$. Pictures refer to horizontal (top), vertical (center) and 45° plane (bottom). [Courtesy O. Napoly]

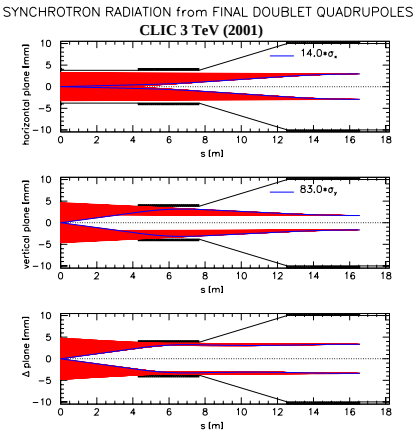

Figure 7: Synchrotron radiation fans for the compact optics with beam envelopes of $14\sigma_x$ and $83\sigma_y$. [O. Napoly]

The collimators are combinations of short (0.5 radiation length) spoilers, made from Be or C, and long (20 r.l.) absorbers. In order that the spoilers are not destroyed by a mis-steered bunch train, the transverse beam area $\sigma_x\sigma_y$ must be larger than (50–100 μm)^2 [9]. For the baseline optics all beam sizes at high-beta points fall between these two limits. The maximum beam sizes in the compact optics are on average a factor 2 smaller. Scaling parts of the NLC collimation design [10] for adequate beam sizes and negligible emittance growth at 1.5 TeV beam energy, we estimate that a separate energy collimation section upstream of the final focus is at least 2 km long. This number assumes that the 2nd set of absorbers as well as the betatron collimation can be integrated into the final focus proper. A complete stand-alone collimation system, as contemplated for NLC, would occupy about 5–6 km, at 1.5 TeV.

A first assessment of muon background was made using a simulation program developed for TESLA [11]. Figure 8 depicts the number of beam particles which must be collimated at various locations along the baseline final focus

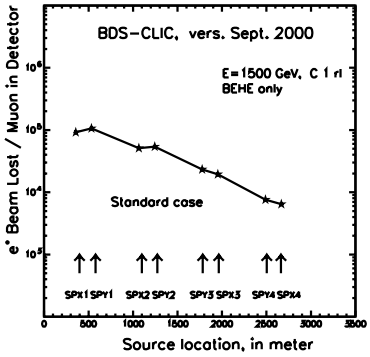

Figure 8: Number of lost electrons per muon passing through a detector with 7.5-m radius as a function of position along baseline final focus. Potential collimator locations are indicated. The IP is at 3282 m.

in order that one muon passes through the detector. At a distance of 500 m from the IP, this number is about 10^4. Lowering the c.m. energy to 500 GeV increases the number of lost beam particles per muon by about an order of magnitude. The dependence on the distance is weak, in Fig. 8. Thus, we do not expect a big difference between the baseline optics and the shorter system. So far only muons generated by the Bethe-Heitler process were considered, and no magnetized toroids or cylinders for muon suppression have yet been included in the final-focus tunnel.

5 CONCLUSION AND THANKS

The compact system [2] provides a larger l^*, a wider momentum bandwidth, and reduced beam tails. Tunability, tolerances and luminosity are comparable to the baseline optics. The horizontal collimation depth is reduced by about a factor of two, due to increased l^* and dispersion across the final doublet. To which extent collimation can be integrated into the two systems remains to be quantified.

We thank O. Napoly for producing Fig. 6, A.-S. Müller for useful discussions and help with PAW, and G. Guignard for a careful reading of the manuscript.

6 REFERENCES

[1] F. Zimmermann, et al., EPAC 2000, Vienna, p. 519.

[2] P. Raimondi and A. Seryi, EPAC 2000, Vienna, p. 492.

[3] K. Oide, HEACC'92, Hamburg, p. 2993 (1992).

[4] H. Grote and F. C. Iselin, CERN-SL-90-13-AP-REV.2.

[5] E. Forest and F. Schmidt, EPAC 2000, Vienna.

[6] F. Schmidt, CERN-SL-94-56-AP; D. P. Barber, G. Ripken and F. Schmidt, DESY 87/036; G. Ripken, DESY-R1-71/1.

[7] O. Napoly, B. Dunham, EPAC 94, London, 1, 698 (1994).

[8] S. Fartoukh, O. Napoly, EPAC98, Stockholm (2000); S. Fartoukh, Ph.D. thesis, DAPNIA/SEA-97-02T (1997).

[9] S. Fartoukh, J.B. Jeanneret, J. Pancin, report in preparation.

[10] P. Tenenbaum et al., LINAC 2000 (2000).

[11] H.J.Schreiber, contribution to ECFA/DESY Workshop Hamburg, 22-25 Sept. 2000.